Catalysis Science & Technology

Accepted Manuscript

ROYAL SOCIETY OF CHEMISTRY

www.rsc.org/catalysis

Comparative study of titanium-functionalized UiO-66: support effect on the oxidation of cyclohexene using hydrogen peroxide

Huong Giang T. Nguyen,[a] Lily Mao,[a] Aaron W. Peters,[a] Cornelius O. Audu,[a] Zachary J. Brown,[a] Omar K. Farha,[a,b,*] Joseph T. Hupp,[a,*] and SonBinh T. Nguyen[a,*]

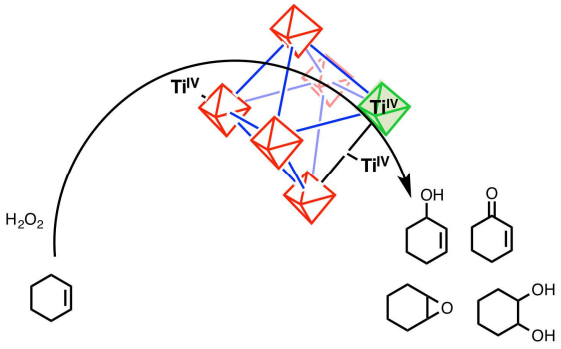

Support effect in UiO-66 with Ti^{IV} as part of nodes, attached to nodes, and on organic linkers is reported.

Catalysis Science & Technology

ARTICLE

Comparative study of titanium-functionalized UiO-66: support effect on the oxidation of cyclohexene using hydrogen peroxide

Received 00th January 20xx,
Accepted 00th January 20xx

DOI: 10.1039/x0xx00000x

www.rsc.org/

Huong Giang T. Nguyen,[a] Lily Mao,[a] Aaron W. Peters,[a] Cornelius O. Audu,[a] Zachary J. Brown,[a] Omar K. Farha,[a,b,*] Joseph T. Hupp,[a,*] and SonBinh T. Nguyen[a,*]

A comparative study of the support effect in three different UiO-66-based MOFs with Ti^{IV} supported as part of the node (UiO-66-Ti_{ex}), attached to the node (Ti-UiO-66), and on a catecholate organic linker (UiO-66-Cat-Ti) is reported. The three MOFs were evaluated for their catalytic activity and selectivity for cyclohexene oxidation. Ti-UiO-66 exhibited greater catalytic turnover numbers than UiO-66-Cat-Ti and UiO-66-Ti_{ex}.

1. Introduction

Metal-organic frameworks (MOFs) are a class of porous and crystalline polymers constructed from inorganic nodes and organic linkers.[1-3] As such, they can support catalytically active metal species either as part of their nodes, attached to their nodes, or ligated to their organic linkers through reactive functionalities at each respective site.[4-12] Given our long-standing efforts in catalysis,[6, 13-19] we were particularly interested in the possibility of supporting catalytically active metal species on available hydroxyl moieties in MOFs, such as those from catechol groups that are part of either an organic ligand[16] or linker[17] and those present on the nodes of the MOF platforms.[15, 20] While each of these strategies has successfully afforded active catalysts on different MOF platforms, the oxidative reactions were quite different in each case, making it difficult to contrast their respective activities and selectivities. Thus, we envisioned that a MOF platform where a catalytically active metal species can be deployed at different sites within the same pore environment can be used as a testing ground for location-dependent effects (or "support effects") on catalysis.

While hydroxyl groups are widely used as sites for anchoring catalytically active metal species onto traditional oxide supports (Al_2O_3, TiO_2, SiO_2, ZrO_2, etc.), the types and distributions of hydroxyl groups on these supports are quite difficult to control. In the most complex case, a support platform can have several types of hydroxyl groups with a broad range of acidities, bridging modes, and densities, all of which can have a significant impact on the catalytic activity and selectivity of the metal species being supported. Specifically, hydroxyl groups with different acidities and surface densities will react and bind to the metal-catalyst precursors in widely diverse manners, affording supported catalyst species with a broad range of coordination environments, activities, and selectivities.[21] These so-called *support effects* are often observed for supported metal oxo and oxide clusters,[22, 23] and are well-known as origins for subtle, difficult-to-control variations in catalyst performance.

In contrast, the crystalline nature of MOFs affords a unique opportunity for deploying hydroxyl groups at different sites on the same MOF platform while maintaining good control on the chemical nature and densities of these groups. In this sense, these hydroxyl groups can behave independently as if they were on different platforms, or domains (i.e., organic, inorganic, interface). Such a MOF can give rise to supported metal species with different catalytic activities and selectivities, similar to that observed for metal-based catalysts supported on different supports.

To our knowledge, "support effects" in MOFs have not been studied by varying the location of the supported metal-based catalyst on the same MOF platform. The advantage in such as system would be a hybrid organic-inorganic approach to anchor single-site catalysts and the ability to tune their electronic environment beyond a simple activity scale in metal oxides. Herein, we report a comparative study of the catalytic activity of UiO-66 functionalized with Ti^{IV} ions as part of the node, attached to the node, and on the organic linker (Scheme 1). The different support sites afforded by this versatile MOF platform engendered Ti^{IV} species with different levels and types of coordinative saturation, which accounted for the large differences in catalytic performance of the three catalysts. As outlined below, our results illustrates that the support effect in MOF-based catalyst is strongly site-dependent and that the coordination environment around the active center should be considered when designing new MOF-based catalysts.

[a] Department of Chemistry and the International Institute for Nanotechnology, Northwestern University, 2145 Sheridan Road, Evanston, Illinois 60208-3113, USA
[b] Department of Chemistry, Faculty of Science, King Abdulaziz University, Jeddah 22254, Saudi Arabia

† Electronic Supplementary Information (ESI) available: MOF characterization data (PXRD, N_2 isotherms, DRIFTS, NMR, SEM, EDS, XPS) and catalysis data. See DOI: 10.1039/c000000x.

Scheme 1. A schematic illustration of Ti^{IV} ions being supported as part of the nodes, on hydroxyl-presenting nodes, and on the catechol-containing struts of UiO-66

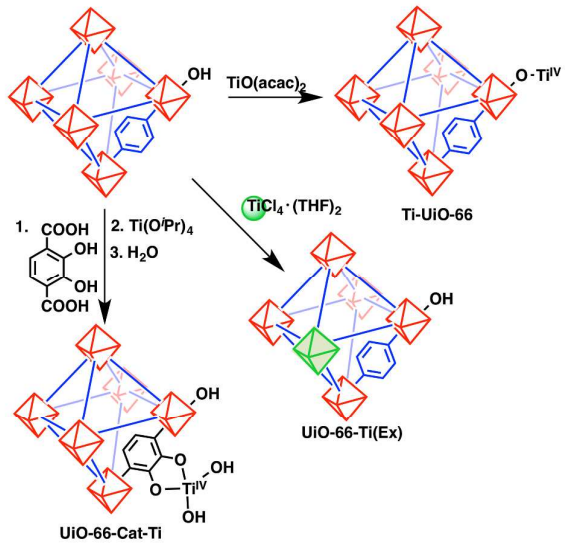

Scheme 2. Potential oxygenated products from the oxidation of cyclohexene.

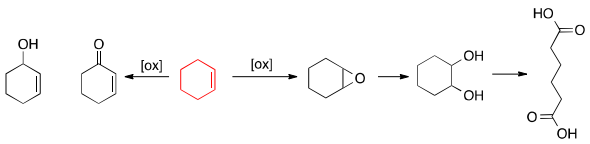

To probe the activity, selectivity, and structure-activity relationships of the differently supported MOF-based metal catalysts, we chose the oxidation of cyclohexene as a model reaction because it can lead to several distinct products (Scheme 2), where their identities depend on the combination of catalyst and oxidant used. For example, radical-mediated oxidation pathways can lead to the allylic-oxidation products 2-cyclohexen-1-ol and 2-cyclohexen-1-one (Scheme 2, left side). Alternatively, the peroxide oxidant can be activated, through binding to the metal center, to undergo reactions with the cyclohexene double bond, affording cyclohexene oxide, which may then undergo a ring-opening reaction in the presence of a nucleophile (such as water) (Scheme 2, right side). We note in passing that while organoperoxides have been used in cyclohexene oxidations, hydrogen peroxide is more desirable as a green oxidant because it yields only water as a side product (and potentially O_2 via decomposition pathways).

A metal-based catalyst that is highly compatible with hydrogen peroxide is titanium silicalite-1 (TS-1), which has hydrophobic channels with Ti^{IV} sites that can catalyze the formation of oxygenated products from linear alkenes and hydrogen peroxide.[24] Part of this activity has been attributed to tetrahedral coordination of the Ti^{IV} ions; in contrast to their octahedral (i.e., coordinatively saturated) analogues, these ions present open coordination sites (potential activation sites) to candidate substrates and/or oxidants.[25, 26] We hypothesized that tetrahedrally coordinated Ti^{IV} ions supported on MOF-based platforms could similarly catalyze the oxidation of cyclohexene with hydrogen peroxide. Additionally, we reasoned that placing Ti^{IV} ions into different coordination environments on the same support platform would allow us to assess and interpret catalytic activity and selectivity in a systematic, deliberate fashion.

We chose UiO-66,[27] a MOF constructed from a 12-coordinated hexazirconium oxo hydroxo cluster and benzene dicarboxylate (BDC), given that both its nodes[15, 28] and struts[29] could be used as "support sites." This MOF is also attractive for oxidation catalysis because it is stable in the presence of hydrogen peroxide oxidant.[29] More importantly for our study, Ti^{IV} ions can be post-synthetically incorporated into UiO-66 at both the nodes and the organic linker sites following literature precedents. First, Cohen and co-workers have reported on the partial exchange of the Zr^{IV} ions *in* the node of UiO-66 with other group IV metals, such as Ti^{IV} or Hf^{IV} ions.[30] Thus, UiO-66-Ti_{ex}, a form of UiO-66 with Ti^{IV} ions partially incorporated as the structural metal (node) is accessible. Second, our groups recently demonstrated that active V^{V} catalyst can be directly incorporated *onto* the hexa-zirconium oxo hydroxo clusters of UiO-66 by reacting with exposed OH groups, especially those that arise from missing linkers.[15] We envisioned that this metallation strategy could be easily generalizable to incorporate other metal ions, including Ti^{IV} ions.

Third, Ti^{IV} ions could also be incorporated on hydroxyl-presenting struts. Our groups[16, 17] and others[29] have synthesized catechol-containing MOFs and used their metallated form for catalysis. Most relevant to the current study is the work by Cohen and coworkers, who utilized linker exchange to synthesize a catechol-containing derivative of UiO-66 that can then be metallated with Fe^{II} and Cr^{III} ions.[29] These metallated materials were found to be active for oxidation catalysis using both *tert*-butyl hydroperoxide and hydrogen peroxide as oxidant.[29] These precedents indicated that Ti^{IV} ions could easily be supported by the struts of a catechol-containing UiO-66. Together, these three PSM strategies provided derivatives of UiO-66 with Ti^{IV} ions being supported under different coordination environment at different sites (Scheme 1), making it possible for us to study the site-dependent support effect in MOFs. As controls, we also examined the activity of TiO_2 and MIL-125-NH_2, a MOF comprising octa-titanium cluster nodes and BDC linkers.[31, 32]

2. Experimental

2.1. Materials and Instrumentation. See Section S1 in the Electronic Supporting Information (ESI)†

2.2. Synthesis of UiO-66, HCl-treated UiO-66, Ti-UiO-66, UiO-66-Cat, UiO-66-Cat-Ti, and UiO-66-Ti_{ex}

UiO-66. This is modification of a protocol reported by Nguyen et al.[15] In a 2 L Erlenmeyer flask, $ZrCl_4$ (1.86 g, 8 mmol)

was dissolved by stirring in DMF (500 mL) and glacial acetic acid (144 g, 137.3 mL, 2.4 mol). In a separate 1 L Erlenmeyer flask, terephthalic acid (1.33 g, 8 mmol) was dissolved completely in DMF (500 mL). This terephthalic acid solution was then added slowly to the $ZrCl_4$ solution and stirred until homogenized. The resulting mixture was partitioned among fifteen 100 mL vials. The vials were capped and heated at 120 °C in an oven for 24 h before being cooled to room temperature. The contents of the vials were combined and the white powder UiO-66 product was collected over a fine-fritted funnel and rinsed with methanol. The collected materials were then immersed in methanol (~35 mL) and kept at 50-60 °C for an additional 24 h. After cooling, this mixture was filtered and air-dried to give a white solid (1.5 g, 70% yield) that was stored at room temperature. Alternatively, the MOF can be activated at 150 °C under high vacuum before being used.

UiO-66-Ti$_{ex}$. UiO-66-Ti$_{ex}$ was made following a literature procedure.[30, 33] Briefly, inside a glovebox and in a 6 dram vial, activated UiO-66 (140 mg) was added to a solution of $TiCl_4(THF)_2$ (170 mg, 0.3 mmol) in anhydrous DMF (10 mL). The vial was capped, taken out of the glove box, and heated at 90 °C in an oven for 5 days. After cooling, the reaction mixture was filtered over a fine-fritted funnel. The collected materials were then quickly rinsed with DMF (3 × 10 mL), removed from the funnel, and immersed in fresh MeOH (~ 10 mL) at 50 °C for 24 h to remove unreacted metal species. After three cycles of soaking, the mixture was filtered and air-dried to give UiO-66-Ti$_{ex}$ with a 0.28 ± 0.01 Ti/Zr content. Samples were activated at 150 °C under high vacuum for 24 h before each catalytic run.

Ti-UiO-66. Inside a glovebox and in a 6 dram vial, activated UiO-66 (250 mg) was added to a solution of $TiO(acac)_2$ (230 mg, 0.75 mmol) in anhydrous MeOH (8 mL). The vial was capped, taken out of the glovebox, and heated at 50 °C in an oil bath for 48 h. After cooling, the reaction mixture was filtered over a fine-fritted funnel. The collected materials were then immersed in fresh MeOH (~10 mL) at 50 °C for 24 h to remove unreacted metal ions. After two cycles of soaking, the mixture was filtered and air-dried to give Ti-UiO-66 Ti/Zr content between 0.04-0.08 (samples used in catalysis had a Ti/Zr content of 0.04). Samples were activated at 150 °C under high vacuum for 24 h before each catalytic run. We note that in our hands $Ti(O^iPr)_4$ is not a good precursor for reacting with UiO-66 in the solution phase: very high (0.71 Ti/Zr molar ratio) Ti loadings was observed, potentially indicative of the formation of TiO_X clusters from condensation side reactions. In contrast, $TiO(acac)_2$ has chelating acac ligands that stabilize it from undergoing condensation, and should be a better precursor for reacting with the hexazirconium oxo hydroxo cluster nodes in a "monomeric" fashion.

UiO-66-Cat. Inside a glovebox and in a 2-5 mL Biotage microwave process vial, activated UiO-66 (45 mg) was added to a solution of 1,2-dihydroxyterephthalic acid (BDC-Cat, 28 mg, 141 µmol) in anhydrous THF (3 mL). The vial was crimped, taken out of the glove box, and heated at 120 °C in an oven for 5 days. After cooling, the reaction mixture was filtered over a fine-fritted funnel. The collected materials were then quickly rinsed with THF (3 × 10 mL) and immersed in fresh THF (~10 mL) at 50 °C for 24 h to remove unreacted ligands. After three cycles of soaking, the mixture was filtered and air-dried to give UiO-66-Cat with 46 mol % BDC-Cat incorporation based on ^{1}H NMR analysis of the sample (after digestion in D_2SO_4). Samples were activated at 150 °C under high vacuum for 24 h before metallation.

UiO-66-Cat-Ti. Activated UiO-66-Cat (~30 mg) was placed in a custom-built stainless steel powder holder and subsequently placed into an atomic layer deposition (ALD) reactor. The sample was allowed to equilibrate for 30 minutes at 120 °C in a 15 sccm (standard cubic centimeters per minute) flow of N_2 before being metallated. The following timing sequence was utilized for the metallation (all times in s): t_1–t_2–t_3 where t_1 is the pulse time of the precursor, t_2 is the exposure time, and t_3 is the purge time. $Ti(O^iPr)_4$ was heated to 90 °C and pulsed (0.2-120-120) 20 times to ensure complete saturation of the coordination sites in the MOF. Distilled water was then pulsed (0.015, 120, 120) 20 times to complete the reaction.

HCl-treated UiO-66 or Ti-UiO-66. In a 6 dram vial, air-dried UiO-66 (or Ti-UiO-66) (~100–200 mg) was added to a mixture of diluted HCl (1 mL of a 8 M solution) and DMF (12 mL) and the resulting suspension was heated either at 50 °C in an oil bath or 100 °C in an oven for 24 h. After cooling, the mixture was filtered over a fine-fritted funnel. The collected solid was resuspended in fresh acetone (~13 mL) and left for 12 h before being decanted and resuspended in fresh acetone (~13 mL) and left for 12 h a second time. The mixture was then filtered and the resulting "decapped" MOF was activated at 150 °C under high vacuum and analyzed with ^{1}H NMR spectroscopy and diffuse reflectance infrared Fourier transform spectroscopy (DRIFTS).

MIL-125-NH$_2$. MIL-125-NH$_2$ was synthesized following a literature protocol.[32] In a 50 mL Erlenmeyer flask, 2-aminoterephthalic acid (560 mg, 3.1 mmol) was dissolved in a mixture of DMF/MeOH (9:1 v/v, 40 mL). $Ti(O^iPr)_4$ (600 µL, 2.03 mmol) was then quickly added and the mixture was stirred and then sonicated in a laboratory bath sonicator (Fisher Scientific model FS6) for an additional 1 minute. The mixture was transferred to a 120 mL telfon-lined Parr acid-digestion vessel. The Parr vessel was sealed and placed into an oven at 150 °C for 24 h. After cooling to room temperature, the Parr vessel was opened and the reaction mixture was filtered over a fine-fritted funnel. The yellow solid product was rinsed with DMF (2 × 10 mL) and MeOH (2 × 10 mL) and allowed to air-dry to give MIL-125-NH$_2$ as a yellow powder. Before catalysis, the MOF was activated under high vacuum at 200 °C for 6 h.

2.3. Catalytic activity evaluation

Catalytic oxidation of cyclohexene. In a 2-5 mL Biotage microwave process vial, either Ti-containing catalyst (2 µmol Ti, 0.1 mol %) or control UiO-66 (13 mg) was added to a mixture of cyclohexene (200 µL, 2 mmol) and naphthalene (25.6 mg, 0.2 mmol, as an internal standard) in acetonitrile (2 mL). Hydrogen peroxide (250 µL of a 30 wt % solution in H_2O)

was then added to the mixture. The reaction vial was capped and placed on a shaker (Thermolyne Maxi-mix III type 65800, set at 200 rpm) equipped with a heating block (set to 50 or 70 °C). After 24 h, the reaction mixture was removed from the shaker and placed into the Eppendorf centrifuge (set at 5 °C) to cool down while the solid MOF was being separated from the reaction mixture via centrifugation. Aliquots (~ 0.02 mL) were then removed from the top part of the reaction mixture, and diluted with DCM (to 1 mL) in a gas chromatography (GC) vial before being analyzed by GC-FID.

Filtration test. After the catalytic oxidation of cyclohexene by Ti-UiO-66 (see the "catalytic oxidation of cyclohexene" section above) had progressed for ~4 h, the microwave vial was removed from the shaker and placed into the centrifuge (set at 5 °C) to cool down while the solid MOF was being separated from the reaction mixture via centrifugation. An aliquot (~0.02 mL) was collected and diluted with DCM (to 1 mL) in a GC vial before being analyzed by GC-FID. Approximately half of the mother liquor was removed via a syringe and filtered through a 0.2 µm PTFE membrane filter into a new microwave vial. The original vial containing the catalyst and the new vial with only the filtrate were then placed back on the shaker and allowed to react for an additional 20 h (for a total of 24 h) and analyzed (as described above) by GC-FID.

Catalyst recycling. Before each recycling experiment, the used catalyst was immersed in acetonitrile (~2 mL), briefly shaken, and let stand undisturbed for 1 h before being separated from the mother liquor by centrifugation. The acetonitrile mother liquor was then gently removed via a syringe to leave the settled catalyst behind; fresh acetonitrile was added; and the immersion-shaken-settling-centrifugation process was repeated twice more to ensure that substrate removal. Then, a new aliquot of substrates and oxidant (as shown above) was added to repeat the catalytic reaction.

H_2O_2 decomposition and temperature stability test. This experiment was carried out following a published protocol,[34] but with a slight modification. Into each J-Young NMR tube, was placed acetonitrile-d_3 (500 µL), chlorobenzene (5 µL as internal standard), and H_2O_2 (30 wt %, 62.5 µL). A sample of the MOF (3.5 mg of UiO-66, 3.5 mg Ti-UiO-66, or 6.8 mg UiO-66-Cat) was then added to each vial. The "blank" does not have any MOF sample added. The J-Young NMR tube was placed into a sand bath at either 50 or 70 °C and ^{1}H NMR spectra were recorded at various time intervals up until 24 h. The peak for H_2O_2 appeared around 9.4 ppm.

3. Results and Discussion

3.1. Synthesis and characterization of Ti-functionalized MOFs

Synthesis of UiO-66-Ti$_{ex}$. UiO-66 was synthesized according to a previously reported literature protocol[15] from a dilute DMF solution of $ZrCl_4$, BDC linker, and acetic acid as the modulator to give octahedral particles ~0.5–1 µm in size (Brunauer–Emmett–Teller (BET) surface area ~1,200 m^2/g, see Figs. S1-S2 in the ESI† for additional characterization data). UiO-66-Ti$_{ex}$ with ~ 22% of Zr^{IV} ions in the node exchanged for Ti^{IV} ions was synthesized from this parent material following previously reported procedures.[30,33] Although in our hands the extent of metal exchange rate was lower than that obtained by Lau *et al.*,[33] the increase in BET surface area of our UiO-66-Ti$_{ex}$ (to 1300 m^2/g, see Fig. S2 in the ESI†) is in agreement with the trend observed by these researchers. The powder X-ray diffraction (PXRD) pattern of the UiO-66-Ti$_{ex}$ was unchanged from that of the parent MOF, indicating the persistence of crystallinity (Fig. S1 in the ESI†).

While the increase in the BET surface area of UiO-66 upon Ti exchange has previously been attributed to the lighter atomic weight of Ti^{IV} compared to Zr^{IV},[33] we hypothesized that the increase in defects that stemmed from the lower maximum coordination number for Ti^{IV} vs. Zr^{IV} (i.e., 6 vs. 8) in the node of UiO-66 also played a significant role.[35, 36] XPS analysis of UiO-66-Ti$_{ex}$ revealed a Ti2p$_{3/2}$ peak at 458.28 eV (Fig. S3 in the ESI†), which is consistent with Ti^{IV} ions in an octahedral coordination environment.[37, 38] A 6-coordinated exchanged-in Ti^{IV} ion cannot bind to the same number of oxo groups, hydroxyl groups, and BDC linkers as the originally present 8-coordinated Zr^{IV} ions (Fig. 1, panel A). In turn, this may result in additional missing linkers, and greater surface area, in the Ti-exchanged version of the MOF. Potentially supporting this hypothesis are scanning electron microscopy (SEM) images of UiO-66-Ti$_{ex}$ (Fig. S4 in the ESI†), which reveal octahedral MOF particles that are significantly roughened relative to those of the parent material. Such changes in morphology might be expected from the defects, stresses, and damages incurred by forcing a 6-coordinated Ti^{IV} ion to replace an 8-coordinated Zr^{IV} ion. Additional evidence for a significant "disturbance" of the node is a shift of the Zr3d peaks in the XPS spectrum of UiO-66-Ti$_{ex}$ to higher binding energy and a small shoulder that arising in the O1s region (Fig. S3 in the ESI†).

As a control sample for Ti^{IV} ions in octahedral coordination environment, we also prepared MIL-125-NH_2, a *de novo-synthesized* Ti-based MOF with BDC-NH_2 struts and octa-titanium oxo hydroxo cluster nodes.[32] As one of the rare MOFs with Ti^{IV} ions, [32,39] MIL-125-NH_2, where the Ti^{IV} ions in the nodes are 6-coordinated, can be isolated as circular plate-like particles with a PXRD pattern matching the simulated pattern and a BET surface area of 1,600 m^2/g (Fig. S6 in the ESI†).

Synthesis of Ti-UiO-66. Ti-UiO-66, where the Ti^{IV} ions are anchored by reacting a Ti^{IV} precursor with the hydroxyl groups on the node of UiO-66, was synthesized by soaking UiO-66 in a methanol solution of TiO(acac)$_2$ for 2 days at 50 °C. The PXRD pattern of the resulting MOF, an off-white solid, matched that of the parent MOF (Fig. S1 in the ESI†) and its BET surface area dropped slightly to 1,080 m^2/g from 1,190 m^2/g (as opposed to

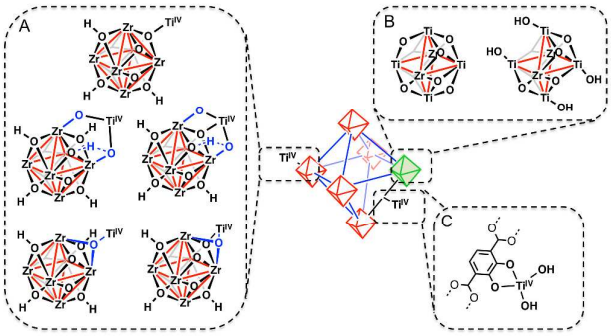

Fig. 1. Proposed structures for Ti^{IV} ions supported on the nodes (A), as the nodes (B), and on the struts (C) of UiO-66. The ligands surrounding these ions are unidentified and thus are omitted.

the increase in BET surface area exhibited by UiO-66-Ti_{ex}) (Fig. S2 in the ESI†). Among the many possible coordination environments for Ti^{IV} ions in this sample (Fig. 1, panel B), a high abundance of tetrahedral Ti^{IV} species with a small contribution from 6-coordinated Ti^{IV} can be inferred through XPS analysis. The $Ti2p_{3/2}$ peak in the XPS spectrum for Ti-UiO-66 is at higher binding energy (458.58 eV) compared to that observed (458.28 eV, see Fig. S3 in the ESI†)) for the octahedral Ti^{IV} species in UiO-66-Ti_{ex}, but not as high as that for tetrahedral Ti^{IV} (458.7 eV).[37] That it is closer to the latter value suggests a composite average of the two species, with a larger contribution from the tetrahedral Ti^{IV}.

Inductively coupled plasma–optical emission spectroscopy (ICP–OES) analysis of Ti-UiO-66 indicated a Ti/Zr molar ratio of ~ 0.04, which is slightly less than that observed (~0.10 molar ratio) for our previous report for V-UiO-66, a UiO-66 derivative that was metallated with $VO(acac)_2$,[15] where the metallation was believed to occur mostly at defect (i.e., missing-linker) sites. For the sample of UiO-66 that is used in this experiment, a micropore volume of 0.44 cm^3/g suggested that ≤1 out of 12 linkers are missing.[40] TGA analysis (Fig. S7 in the ESI†) supports this assessment[41] and implies that the number of missing BDC linkers is ~0.6 out of 12, (~5% of the total linkers). Based on that value, we anticipated that up to ~10 mol % of the organic ligands in the MOF could be acetate ions, which "cap" these missing-linker sites, and thus up to a ~0.10 Ti/Zr molar ratio (maximum value for metallation at all defect sites) seems possible.

Multiple factors may account for the observation that metallation is lower than 10%. First, $TiO(acac)_2$ can exist as a dimer,[42, 43] an entity that is too large to fully infiltrate the MOF crystal. While it is possible that monomeric $Ti(OR)_4$ can be formed from the reaction of the $TiO(acac)_2$ dimer with methanol over the course of the metallation reaction, the concentration of monomeric complex is likely too low[44] for the monomer to play a major role in metallation. Second, the known facile exchange of the ligands on $Ti^{IV}(OR)_{4-x}(acac)_x$ with alcohols[44] suggests that the post-synthetically installed Ti^{IV} may subsequently detach from the hexazirconium oxo hydroxo cluster if exposed to competitive ligands. Related to this suggestion is the experimental observation (see additional discussion below) that Ti-UiO-66 samples can easily lose Ti^{IV} ions upon treatment with dilute acid.[45]

Treating UiO-66 and Ti-UiO-66 with a dilute solution of HCl, to replace the acetate capping ligands,[15] further supported the notion that the latter sample is not fully metallated. Both HCl-treated samples exhibit a peak around 3773 cm^{-1} in their DRIFTS spectra (Fig. S9 in the ESI†) that is attributed to the terminal OH groups of missing-linker sites.[30, 46] However, the intensity of this peak is lower in the spectrum of the HCl-treated Ti-UiO-66 sample compared to that for the HCl-treated UiO-66 sample, consistent with our earlier supposition that *some, but not all*, of the defect sites have reacted with Ti^{IV} ions. This result, however, could also be partially attributed to the 25% loss of metal loading in HCl-treated Ti-UiO-66 (0.03 Ti/Zr molar ratio from the initial 0.04) after HCl treatment, as determined by ICP-OES analysis. As discussed above, this lability is consistent with the known facile exchange of the ligands on $Ti^{IV}(OR)_{4-x}(acac)_x$ with alcohols.[44]

Synthesis of UiO-66-Cat-Ti. UiO-66-Cat-Ti was synthesized by ALD metallation of UiO-66-Cat, which was made from UiO-66 by exchanging out BDC with BDC-Cat in THF.[47] Soaking the parent UiO-66 in a THF solution of BDC-Cat at 120 °C for 5 days led to ~46% exchange of the BDC linker for BDC-Cat based on analysis of the ^1H NMR spectrum of UiO-66-Cat (after digestion in D_2SO_4) (Fig. S10 in the ESI†). ^1H NMR analysis of the filtrate showed the expected release of BDC (~52%) into the solution, further indicating that BDC-Cat was not simply trapped inside the pores of UiO-66 and that an exchange indeed did take place. In addition, XPS analysis of UiO-66-Cat indicated a small shift in the binding energy of the Zr3d peaks (from 185.08 and 182.78 eV to 185.28 and 182.88 eV, respectively) (Fig. S3 in the ESI†), which would be expected if Zr^{IV} was bound to BDC-Cat, a ligand that is more electron-donating than BDC. As expected from the incorporation of the bulkier catecholated linker, as well as the possibility of the BDC-Cat struts filling in the small fraction of missing linker sites, a lower BET surface area (900 m^2/g) was observed for UiO-66-Cat.

UiO-66-Cat could be easily metallated with $Ti(O^iPr)_4$ vapor to yield UiO-66-Cat-Ti with 0.03 ± 0.01 molar ratio of Ti/Zr. The small amount of metal loading compared to catechol incorporation could be attributed to mostly surface metallation as the dimensions of $Ti(O^iPr)_4$ are much larger than the pore apertures of < 6 Å expected for UiO-66-Cat. Consequently, only a small decrease in the BET surface area to 830 m^2/g was observed (Fig. S2 in the ESI†). XPS analysis of UiO-66-Cat-Ti shows a $Ti2p_{3/2}$ peak at 458.78 eV binding energy (Fig. S3 in the ESI†), suggesting an even higher proportion of tetrahedral Ti^{IV} species in this sample compared to Ti-UiO-66.[37] We note that the integrity of the UiO-66 framework was maintained through both post-synthesis modification steps as indicated by the PXRD pattern and SEM images (Figs. S1 and S4 in the ESI†).

3.2. Cyclohexene oxidation

The oxidation of cyclohexene was carried out in acetonitrile at either 50 or 70 °C and in the presence of 0.1 mol

Scheme 3. The oxidation of cyclohexene with hydrogen peroxide and Ti-functionalized UiO-66 catalysts

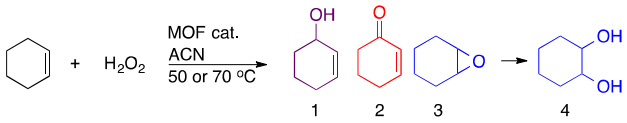

Table 1. TONs for various cyclohexene-oxidation products using different Ti-functionalized UiO-66 catalysts (0.1 mol % Ti, at either 50 or 70 °C)

Entry	Catalyst	Temp (°C)	TON[a] (mol product/mol catalyst) **3** (**4**)[c]	**1**	**2**
1	Ti-UiO-66	50	7	20	66
2	UiO-66-Ti_{ex}	50	3	4	8
3	UiO-66-Cat-Ti	50	0	1	2
4	MIL-125-NH_2	50	1	1	3
5	UiO-66	50	3	3	8
6	No catalyst	50	30[b]	0[b]	0[b]
7	TiO_2	50	29	0	0
8	Ti-UiO-66	70	3 (15)	48	205
9	UiO-66-Ti_{ex}	70	7	20	81
10	UiO-66-Cat-Ti	70	(10)	14	39
11	MIL-125-NH_2	70	6	23	100
12	UiO-66-Cat	70	0	0	0
13	UiO-66	70	3	33	90
14	No catalyst	70	106[b]	4[b]	6[b]
15	TiO_2	70	87	3	7
16	$TiO(acac)_2$	50	3.5	11	45
17	$TiO(acac)_2$	70	7	22	79

[a]Because a small percentage of the cyclohexene was lost due to evaporation and from being trapped inside the MOF after catalysis (as determined by ^{1}H NMR analysis of the digested MOF), TON was calculated based on the amount of products being formed (instead of the amount of cyclohexene being consumed). [b]For purpose of comparison, the TON is calculated assuming that 0.1 mol % of some Ti species is present. [c]The diol is presumed to arise from the ring-opening of the epoxide by water, which can be catalysed by either a Lewis (in the case of Ti-UiO-66) or Brønsted (in the case of UiO-66-Cat-Ti) acid.

% of catalyst with hydrogen peroxide as the oxidant (Scheme 3). The reaction was evaluated by gas chromatography after 24 h and the results are summarized in Table 1. As expected, no conversion was observed at room temperature. However, a small amount of cyclohexene oxide can still be formed at elevated temperature in the absence of any catalyst (~3 mol % at 50 °C and ~10 mol % at 70 °C, respectively, Table 1, cf. entries 6 and 14).

Notwithstanding the aforementioned background reaction, the presence of Ti-functionalized MOF catalysts led to dramatic changes in activity and product selectivity, favouring the allylic oxidation products over the epoxide. Interestingly, control experiments with UiO-66 yielded a different product profile comparing to that of the blank (Table 1, cf. entries 5 vs 6 and 13 vs 14), suggesting that the Zr cluster node might have some, albeit minimal, oxidation activity. Nevertheless, the higher TON for Ti-UiO-66 confirms that Ti^{IV} ions are responsible for the catalytic activity. Indeed, Ti-UiO-66 is the most active of the three Ti-functionalized MOF catalysts at both 50 and 70 °C. While UiO-66-Ti_{ex} appears to have slightly higher catalytic activity than UiO-66-Cat-Ti at both temperatures, both product profiles resemble those of Ti-UiO-66 in affording mostly alcohol and ketone. Based on the total TONs alone, the observed order in catalytic performance is: Ti-UiO-66 >> UiO-66-Ti_{ex} ~ MIL-125-NH_2 > UiO-66-Cat-Ti. This is not consistent with the expected coordination environment of the Ti^{IV} catalyst in the different MOF systems, as discussed above (Fig. 1). However, when the activity of UiO-66-Cat-Ti is compared to that of the unmetallated UiO-66-Cat, which is essentially unproductive, the catalysis that can be attributed to the presence of Ti^{IV} species exceeds that of the {UiO-66-Ti_{ex}/UiO-66} pair (Table 5.1, cf. entries 10 vs 12 and entries 9 vs 13). Based on these data, the corrected trend of activity for our three UiO-66-based catalysts is then: Ti-UiO-66 >> UiO-66-Cat-Ti > UiO-66-Ti_{ex}, which supports our original hypothesis that tetrahedral Ti^{IV} ions should be more active than the more saturated octahedral Ti^{IV} ions. The octahedral Ti^{IV} centers in MIL-125-NH_2 should be minimally active because they have no coordination site for the binding of oxidant or substrate. This is the same situation for the Ti^{IV} ions in UiO-66-Ti_{ex}, which are also expected to be coordinatively saturated. As a result, the catalytic activities in both of these cases are quite similar to that of the parent UiO-66.[48] Further supporting this hypothesis is the observation that adding catechol (20 mol %) to Ti-UiO-66 afforded no cyclohexene oxygenated products, presumably due to the "poisoning" of the tetrahedral Ti^{IV} centers by catechol binding, which creates inactive octahedral Ti^{IV} sites.

In the absence of substrate, the decomposition of H_2O_2 at 70 °C follows the order Ti-UiO-66 > UiO-66-Cat-Ti ~ UiO-Ti_{ex} > UiO-66 > UiO-66-Cat > blank (Figs. S12-S13 in the ESI†), again consistent with the corrected activity trend. Nevertheless, the oxidation of cyclohexene can still be competitive against H_2O_2 decomposition for Ti-UiO-66 (H_2O_2 productivity is ~50%).[49] Interestingly, the presence of the BDC-Cat linker in UiO-66-Cat seems to slow down H_2O_2 decomposition in comparison to UiO-66, as well as prevent all background reaction in cyclohexene oxidation.

Since Ti-UiO-66 is the most active of the Ti-based UiO-66 catalysts, we evaluated it for heterogeneity and recyclability. A filtration test on a Ti-UiO-66-catalyzed reaction mixture after 4 h of catalysis showed that there is little additional catalysis in the filtrate (beyond background conversion), confirming that the catalysis is mostly heterogeneous. Unfortunately, the catalyst progressively lost its activity at both 70 °C and 50 °C, retaining only 75% of activity during the 3rd cycle at 70 °C and exhibiting almost no catalytic activity beyond background during the 3rd cycle at 50 °C. ICP–OES analysis of the MOF after 3 cycles of catalysis at 50 °C indicated that ~1/3 of the metal was lost, suggesting that the catalyst could be partially deactivated through metal leaching. We note that leaching of Ti^{IV} ions from MCM-41 support has been reported when aqueous hydrogen peroxide is used as an oxidant.[50] To ensure that TiO_2 nanoparticles do not contribute to the observed catalysis, we also examined the activity of 20 nm TiO_2 particles

as a control. The TiO_2 nanoparticle has 100% selectivity for the epoxide and gave similarly low conversion (2.9%, 29 TON) to that of the blank (Table 1, cf. entries 7 vs 6 and 15 vs 14), suggesting that the TiO_2 nanoparticles, if any are formed, do not contribute significantly to the observed catalytic activity.

4. Conclusions

In summary, we have explored the support effect in the UiO-66 MOF platform through three different Ti-based catalysts. Ti^{IV} ions were supported either as part of the nodes, attached to the nodes, or on the struts of the UiO-66 platform. While the Ti^{IV} ions in these catalysts are all supported by oxygen-based ligands, their activities and selectivities varied dramatically, with Ti^{IV} ions supported at sites that can foster tetrahedral coordination of Ti^{IV} yielding the more active catalysts, and Ti-UiO-66 being most active. These results underscore the importance of considering site-dependent support effects when designing new MOF-based catalysts.

5. Acknowledgments

This work was supported by the Chemical Sciences, Geosciences, and Biosciences Division, US Department of Energy through a grant (DE FG02-03ER15457) to the Institute of Catalysis for Energy Processes (ICEP) at Northwestern University (assistantship for H.G.T.N). A.W.P. acknowledges support from the Department of Defense through the National Defense Science & Engineering Graduate Fellowship (NDSEG) Program. C.O.A. acknowledges support from the National Science Foundation (NSF) Graduate Research Fellowships Program (GRFP). L.M. is supported by an NSF-DMREF grant (Award No. CMMI-1235480). This work made use of the Clean Catalysis Facility of Northwestern University Center for Catalysis and Surface Science, which acknowledges funding from the Department of Energy (DE-FG02-03ER15457 and DE-AC02-06CH11357) used for the purchase of the Thermo Nicolet/Harrick DRIFTS system. Experimental facilities at the Integrated Molecular Structure Education and Research Center (IMSERC), J. B. Cohen X-Ray Diffraction Facility at the Materials Research Center, Keck II Facility and the Northwestern University Atomic- and Nanoscale Characterization Experimental Center (EPIC) of NU*ANCE* Center at Northwestern University are supported by the International Institute for Nanotechnology, NSF-MRSEC (NSF DMR-1121262), the Keck Foundation, the state of Illinois, and Northwestern University.

6. Notes and references

1. O. M. Yaghi, M. O'Keeffe, N. W. Ockwig, H. K. Chae and J. Kim, *Nature*, 2003, **423**, 705-714.
2. G. Férey, *Chem. Soc. Rev.*, 2008, **37**, 191-214.
3. S. Kitagawa, R. Kitaura and S.-i. Noro, *Angew. Chem., Int. Ed.*, 2004, **43**, 2334-2375.
4. A. Corma, H. Garcia and F. X. Llabrés i Xamena, *Chem. Rev.*, 2010, **110**, 4606-4655.
5. J. Gascon, A. Corma, F. Kapteijn and F. X. Llabrés i Xamena, *ACS Catal.*, 2013, **4**, 361-378.
6. J. Lee, O. K. Farha, J. Roberts, K. A. Scheidt, S. T. Nguyen and J. T. Hupp, *Chem. Soc. Rev.*, 2009, **38**, 1450-1459.
7. Z.-Y. Gu, J. Park, A. Raiff, Z. Wei and H.-C. Zhou, *ChemCatChem*, 2014, **6**, 67-75.
8. K. Manna, T. Zhang, M. Carboni, C. W. Abney and W. Lin, *J. Am. Chem. Soc.*, 2014, **136**, 13182-13185.
9. H.-S. Lu, L. Bai, W.-W. Xiong, P. Li, J. Ding, G. Zhang, T. Wu, Y. Zhao, J.-M. Lee, Y. Yang, B. Geng and Q. Zhang, *Inorg. Chem.*, 2014, **53**, 8529-8537.
10. J. Gao, L. Bai, Q. Zhang, Y. Li, G. Rakesh, J.-M. Lee, Y. Yang and Q. Zhang, *Dalton Trans.*, 2014, **43**, 2559-2565.
11. F. Song, T. Zhang, C. Wang and W. Lin, *Proc. R. Soc. A,* **2012***, 468,* 2035-2052.
12. K. Manna, T. Zhang and W. Lin, *J. Am. Chem. Soc.*, 2014, **136**, 6566-6569.
13. S.-H. Cho, B. Ma, S. T. Nguyen, J. T. Hupp and T. E. Albrecht-Schmitt, *Chem. Commun.*, 2006, **42**, 2563-2565.
14. O. K. Farha, A. M. Shultz, A. A. Sarjeant, S. T. Nguyen and J. T. Hupp, *J. Am. Chem. Soc.*, 2011, **133**, 5652-5655.
15. H. G. T. Nguyen, N. M. Schweitzer, C.-Y. Chang, T. L. Drake, M. C. So, P. C. Stair, O. K. Farha, J. T. Hupp and S. T. Nguyen, *ACS Catal.*, 2014, **4**, 2496-2500.
16. H. G. T. Nguyen, M. H. Weston, O. K. Farha, J. T. Hupp and S. T. Nguyen, *CrystEngComm*, 2012, **14**, 4115-4118.
17. H. G. T. Nguyen, M. H. Weston, A. A. Sarjeant, D. M. Gardner, Z. An, R. Carmieli, M. R. Wasielewski, O. K. Farha, J. T. Hupp and S. T. Nguyen, *Cryst. Growth Des.*, 2013, **13**, 3528-3534.
18. A. M. Shultz, O. K. Farha, J. T. Hupp and S. T. Nguyen, *J. Am. Chem. Soc.*, 2009, **131**, 4204-4205.
19. A. M. Shultz, A. A. Sarjeant, O. K. Farha, J. T. Hupp and S. T. Nguyen, *J. Am. Chem. Soc.*, 2011, **133**, 13252-13255.
20. J. E. Mondloch, W. Bury, D. Fairen-Jimenez, S. Kwon, E. J. DeMarco, M. H. Weston, A. A. Sarjeant, S. T. Nguyen, P. C. Stair, R. Q. Snurr, O. K. Farha and J. T. Hupp, *J. Am. Chem. Soc.*, 2013, **135**, 10294-10297.
21. M. Breysse, P. Afanasiev, C. Geantet and M. Vrinat, *Catal. Today*, 2003, **86**, 5-16.
22. L. J. Burcham and I. E. Wachs, *Catal. Today*, 1999, **49**, 467-484.
23. X.-B. Han, Z.-M. Zhang, T. Zhang, Y.-G. Li, W. Lin, W. You, Z.-M. Su and E.-B. Wang, *J. Am. Chem. Soc.*, 2014, **136**, 5359-5366.
24. B. Notari, *Catal. Today*, 1993, **18**, 163-172.
25. H. Nur, *Mater. Sci. Eng., B*, 2006, **133**, 49-54.
26. B. Notari, *Adv. Catal.*, 1996, **41**, 253-334.
27. J. H. Cavka, S. Jakobsen, U. Olsbye, N. Guillou, C. Lamberti, S. Bordiga and K. P. Lillerud, *J. Am. Chem. Soc.*, 2008, **130**, 13850-13851.
28. C. Larabi and E. A. Quadrelli, *Eur. J. Inorg. Chem.*, 2012, **2012**, 3014-3022.
29. H. Fei, J. Shin, Y. S. Meng, M. Adelhardt, J. Sutter, K. Meyer and S. M. Cohen, *J. Am. Chem. Soc.*, 2014, **136**, 4965-4973.

30. M. Kim, J. F. Cahill, H. Fei, K. A. Prather and S. M. Cohen, *J. Am. Chem. Soc.*, 2012, **134**, 18082-18088.
31. C. Zlotea, D. Phanon, M. Mazaj, D. Heurtaux, V. Guillerm, C. Serre, P. Horcajada, T. Devic, E. Magnier, F. Cuevas, G. Ferey, P. L. Llewellyn and M. Latroche, *Dalton Trans.*, 2011, **40**, 4879-4881.
32. S. Hu, M. Liu, K. Li, Y. Zuo, A. Zhang, C. Song, G. Zhang and X. Guo, *CrystEngComm*, 2014, **16**, 9645-9650.
33. C. Hon Lau, R. Babarao and M. R. Hill, *Chem. Commun.*, 2013, **49**, 3634-3636.
34. C. W. Yoon, K. F. Hirsekorn, M. L. Neidig, X. Yang and T. D. Tilley, *ACS Catal.*, 2011, **1**, 1665-1678.
35. U. Schubert, *Chem. Mater.*, 2001, **13**, 3487-3494.
36. U. Schubert, *J. Mater. Chem.*, 2005, **15**, 3701-3715.
37. M. A. Arillo, M. L. Lopez, M. L. Pico, A. Veiga, A. Jimenez-Lopez and E. Rodriguez-Castellon, *J. Alloys Compd.*, 2001, **320**, 160-163.
38. M. Murata, K. Wakino and S. Ikeda, *J. Electron Spectrosc. Relat. Phenom.*, 1975, **6**, 459-464.
39. J. Gao, J. Miao, P.-Z. Li, W. Y. Teng, L. Yang, Y. Zhao, B. Liu and Q. Zhang, *Chem. Commun.*, 2014, **50**, 3786-3788.
40. H. Wu, Y. S. Chua, V. Krungleviciute, M. Tyagi, P. Chen, T. Yildirim and W. Zhou, *J. Am. Chem. Soc.*, 2013, **135**, 10525-10532.
41. F. Vermoortele, M. Vandichel, B. Van de Voorde, R. Ameloot, M. Waroquier, V. Van Speybroeck and D. E. De Vos, *Angew. Chem., Int. Ed.*, 2012, **51**, 4887-4890.
42. M. Pathak, R. Bohra, R. Mehrotra, I.-P. Lorenz and H. Piotrowski, *Transition Met. Chem.*, 2003, **28**, 187-192.
43. G. D. Smith, C. N. Caughlan and J. A. Campbell, *Inorg. Chem.*, 1972, **11**, 2989-2993.
44. R. J. Errington, J. Ridland, W. Clegg, R. A. Coxall and J. M. Sherwood, *Polyhedron*, 1998, **17**, 659-674.
45. Based on the fact that elemental analysis of UiO-66 shows a very small Cl content, we ruled out the possibility that the defect sites of the UiO66 nodes are capped by Cl^- ions (instead of OH or H_2O) and thus are unavailable for reaction with the $TiO(acac)_2$ precursors.
46. J. Nawrocki, M. Rigney, A. McCormick and P. W. Carr, *J. Chromatogr. A*, 1993, **657**, 229-282.
47. We note in passing that while Cohen and co-workers was able to synthesize UiO-66-Cat by in DMF or water (see reference29), this procedure did not work in our hands.
48. We note in passing that we cannot rule out the possibility that UiO-66-Ti_{ex} and MIL-125-NH_2 can decompose hydrogen peroxide via some undetermined path ways. See further discussion in the next paragraph.
49. The H_2O_2 productivity is defined as the amount of oxidant equivalent that is channelled into productive oxidation pathways. It is less <30% for the remaining catalyst systems.
50. C. Rhee and J. Lee, *Catal. Lett.*, 1996, **40**, 261-264.